Toxicology and Applied Pharmacology 280 (2014) 484–492

Contents lists available at ScienceDirect

Toxicology and Applied Pharmacology

journal homepage: www.elsevier.com/locate/ytaap

# Biodistribution and toxicological study of PEGylated single-wall carbon nanotubes in the zebrafish (*Danio rerio*) nervous system

Gisele E.B. Weber [a,b], Lidiane Dal Bosco [a,b], Carla O.F. Gonçalves [c], Adelina P. Santos [c], Cristiano Fantini [d], Clascídia A. Furtado [c], Gustavo M. Parfitt [a,b], Carolina Peixoto [a,b], Luis Alberto Romano [e], Bernardo S. Vaz [a,b], Daniela M. Barros [a,b,*]

[a] Laboratório de Neurociências, Instituto de Ciências Biológicas, Universidade Federal do Rio Grande (FURG), Rio Grande, RS, 96210-900, Brazil
[b] Programa de Pós-graduação em Ciências Fisiológicas–Fisiologia Animal Comparada, FURG, Rio Grande, RS, 96210-900, Brazil
[c] Laboratório de Química de Nanoestruturas, Centro de Desenvolvimento da Tecnologia Nuclear, Belo Horizonte, MG, 31270-901, Brazil
[d] Instituto de Ciências Exatas, Departamento de Física, Belo Horizonte, MG, 31270-901, Brazil
[e] Instituto de Oceanografía, Universidade Federal do Rio Grande, Rio Grande, RS, 96210-030, Brazil

ARTICLE INFO

*Article history:*
Received 6 March 2014
Revised 9 August 2014
Accepted 15 August 2014
Available online 26 August 2014

*Keywords:*
SWNT-PEG
Biocompatibility
Biodistribution
Behavioral
Oxidative stress
Toxicity

ABSTRACT

Nanotechnology has been proven to be increasingly compatible with pharmacological and biomedical applications. Therefore, we evaluated the biological interactions of single-wall carbon nanotubes functionalized with polyethylene glycol (SWNT-PEG). For this purpose, we analyzed biochemical, histological, behavioral and biodistribution parameters to understand how this material behaves *in vitro* and *in vivo* using the fish *Danio rerio* (zebrafish) as a biological model. The *in vitro* results for fish brain homogenates indicated that SWNT-PEG had an effect on lipid peroxidation and GSH (reduced glutathione) content. However, after intraperitoneal exposure, SWNT-PEG proved to be less biocompatible and formed aggregates, suggesting that the PEG used for the nanoparticle functionalization was of an inappropriate size for maintaining product stability in a biological environment. This problem with functionalization may have contributed to the low or practically absent biodistribution of SWNT-PEG in zebrafish tissues, as verified by Raman spectroscopy. There was an accumulation of material in the abdominal cavity that led to inflammation and behavioral disturbances, as evaluated by a histological analysis and an open field test, respectively. These results provide evidence of a lack of biocompatibility of SWNTs modified with short chain PEGs, which leads to the accumulation of the material, tissue damage and behavioral alterations in the tested subjects.



## Introduction

Nanomaterials, including single-wall carbon nanotubes, possess chemical, physical and/or biological properties that are dependent on the nanostructure and that provide functional characteristics of interest for applications in the biomedical field (Oberdörster et al., 2005; Zhao et al., 2011). These nanomaterials can interact with biological systems at the molecular and supramolecular levels with high specificity (Smith and Mizumori, 2006; Gilmore et al., 2008; Cheung et al., 2010; Meng et al., 2012). In recent years, numerous studies have been conducted to evaluate the potential applications of carbon nanotube devices for diagnostics, the transport and controlled release of drugs and cell culture (Kam et al., 2005; Medina et al., 2007; Foldvari and Bagonluri, 2008; Liang and Chen, 2010; Vashist et al., 2011; Naderi et al., 2013).

Strategies for carbon nanotube purification and for controlling their dispersion and stability in physiological media are required to optimize these nanoparticles for biomedical applications (Ajayan, 1999). Their high hydrophobicity and tendency to form aggregates in aqueous media are challenges that must be overcome. One of the main strategies to solving these issues is to modify the NT surfaces with appropriate chemical moieties, such as hydrophilic polymers (Liu et al., 2009). Thus, the incorporation of polyethylene glycol (PEG) has become an attractive option for biological applications, as it not only improves NT dispersibility and stability in physiological media but also provides the particles with a biocompatible and protective surface, increasing the blood circulation half-life and decreasing the liver uptake of these nanostructures (Liu et al., 2009; Yang et al., 2008, 2008b; Ilbasmiş-Tamer et al., 2010).

Carbon nanotubes functionalized with polyethylene glycol (SWNT-PEG) have various applications in the biomedical field; however, this work is focused on their applications in nervous tissue. The neuroprotective effects of SWNT-PEG *in vivo* were first reported by Roman et al. (2011), who demonstrated their actions on axonal repair

* Corresponding author at: Laboratório de Neurociências, Instituto de Ciências Biológicas, Universidade Federal do Rio Grande (FURG), Av Itália, Km 8, Rio Grande, RS, 96210-900, Brazil.
*E-mail address:* barrosdm@yahoo.com.br (D.M. Barros).

http://dx.doi.org/10.1016/j.taap.2014.08.018
0041-008X/

and functional recovery in rats after spinal cord injury. Therefore, neuroscience is a promising field for nanotechnology applications, especially for devices and materials based on NTs (Smith and Mizumori, 2006). Studies have demonstrated the biocompatibility of NT-containing substrates based on the ability of nerve cells to grow and differentiate (Mattson et al., 2000; Liopo et al., 2006; Galvan-Garcia et al., 2007). Moreover, changes in the NT structure may modulate the development of neurons in culture (Bekyarova et al., 2005; Sucapane et al., 2009). Although the aforementioned studies may report exciting applications for NTs in neuroscience, other reports have shown some drawbacks related to their application. Because the internalization of nanoparticles, in some cases, triggers reactions that lead to cell death (Nel et al., 2006; Porter et al., 2007), an investigation of the potential toxic effects arising from interactions between the NT and cellular constituents is of fundamental importance for its medical application.

Because the neurochemical systems and neural structures of zebrafish have many similarities to those of other vertebrates, it is an important biological model for studying neurotoxicology (Linney et al., 2004; Barros et al., 2008; de Castro et al., 2009), including assessing the behavioral and biochemical effects of nanomaterials (Fako and Furgeson, 2009).

Determining the biodistribution and accumulation of nanomaterials in the different organs and tissues of exposed organisms should also be considered necessary for a comprehensive toxicological study. NTs that reach the CNS are known to promote oxidative stress (Nel et al., 2006; Oberdörster et al., 2009). Additionally, NTs can accumulate in tissues and cause neuronal injury (Zhang et al., 2010), which implies functional damage to the exposed organisms. Depending on their surface modifications and physicochemical characteristics, NTs may exhibit distinct patterns of biodistribution, toxicity and accumulation in the organs of exposed organisms (Cheng et al., 2009; Kang et al., 2009; Johnston et al., 2010; Jain et al., 2011).

Therefore, the aim of the present work was to investigate the possible *in vitro* and *in vivo* effects of SWNT-PEG in *Danio rerio* "zebrafish" (Teleostei, Cyprinidae). To evaluate if the SWNT-PEG exposition leads to oxidative damage or interacts with the antioxidant machinery, we used an *in vitro* system of the zebrafish nervous system. Hereafter, to evaluate the biodistribution and possible behavioral alterations, intact animals were exposed intraperitoneally to SWNT-PEG dispersions, and to characterize the consequences of the apparent bioaccumulation, histological analyses of the target tissues (organs of the abdominal cavity and the brain) were performed.

## Experimental section

### *Preparation of SWNT-PEG dispersion and sample characterization*

In the present study, we used a commercial sample of single-wall carbon nanotubes (SWNTs) (Sigma-Aldrich, 652474, Lot MKBC 9435,

| | SWNT-PEG |
|---|---|
| TEM Image | 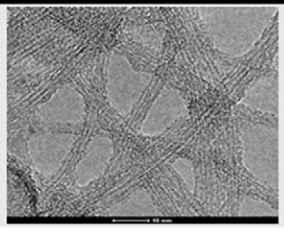 |
| Size Distribution | 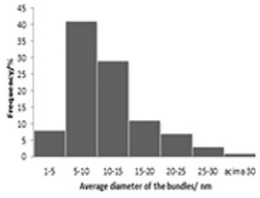  |
| Diameter (nm) | 1-30 |
| Length (nm) | 200-2000 |
| SWNT | 60 wt% |
| SWNT-PEG | 25 wt% |
| 20-40 nm diameter carbon-coated catalyst particles (Ni – Y) | 20 wt% |

**Fig. 1.** Physical and chemical characterization of SWNT-PEG. The size distribution, surface coating and purities were characterized using the various techniques described in the Experimental Section.

St. Louis, MO, USA) synthesized via the electric arc discharge method and functionalized with polyethylene glycol (PEG, MW = 600 Da). The SWNT-PEG material provided was found to contain ~25 wt.% of grafted PEG, ~60 wt.% of SWNTs and ~20 wt.% of 20–40 nm diameter carbon-coated catalyst particles (Ni–Y), as determined by thermogravimetric (TGA) (TA Instruments, SDT 2960, in dry air at a scanning rate of 5 °C $min^{-1}$) and transmission electron microscopic (TEM) (FEI, Tecnai G2-20 SuperTwin, 200 kV) analyses.

An SWNT-PEG dispersion was prepared in deionized water at a high concentration (greater than 2 mg/ml). To prepare a stable dispersion and remove excess unbound PEG, a multi-step dispersion process employing several cycles of sonication, high-shear mixing, centrifugation and ultracentrifugation was required. The procedure was adapted from Kalinina et al. (2011).

The morphological characteristics of the dispersion were analyzed by TEM and high-resolution TEM (HRTEM) performed on a FEI Tecnai G2-Spirit 120-kV and a FEI Tecnai G2-20 SuperTwin 200-kV microscope, respectively. AFM (atomic force microscopy) observations were carried out with an NTegra Aura (NT-MDT Co.) microscope. The Zeta potential was determined using the electrophoretic light scattering technique on a Zetasizer Nano-ZS ZEN3600 system (Malvern Instruments). The final concentration of SWNTs in the dispersion was spectrophotometrically evaluated by performing optical absorption measurements using a Shimadzu UV–Vis–NIR spectrophotometer UV-3600 over the wavelength range of 190 to 1100 nm. A standard curve of the absorbance *vs.* SWNT concentration (based on the Lambert-Beer law) was generated by diluting the original dispersion in water and measuring the optical absorbance at 700 nm. The mass concentration was determined by drying and weighing a known volume of the original dispersion.

## *In vitro experiments*

*Animals and housing.* Five hundred adult "wild type" (short fin) zebrafish (*D. rerio*) were obtained through breeding and cultivation in aquariums in an aquatic bioterium room at the Institute of Biological Sciences ,ICB, FURG or from a commercial supplier (Red Fish, Porto Alegre, RS, Brazil). All fish were acclimated for at least 2 weeks in the experimental room, were housed in groups of 15 fish in 15 L and were kept in a recirculating water system equipped with a biological filter and disinfected using UV light with controlled temperature (28 ± 2 °C), pH (7) and a 14–10 h day/night photoperiod. Feeding was performed using a balanced artificial diet (Tetra Color Tropical Granules) offered *ad libitum* twice daily. All protocols were approved by the Institutional Animal Care Committee (process number 029/2011, CEUA-FURG) and followed Brazilian legislation, the guidelines of the Brazilian Collegium of Animal Experimentation (COBEA) and the Canadian Council for Animal Care (CCAC) "Guide on the Care and Use of Fish in Research, Teaching and Testing."

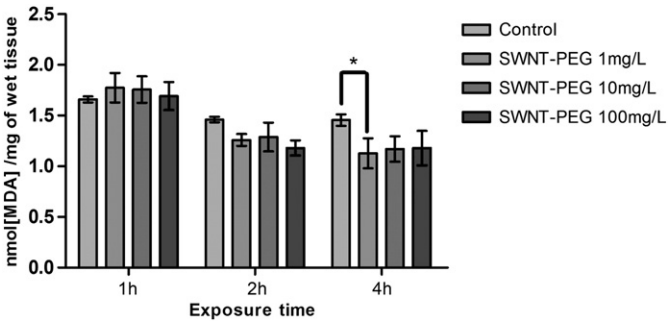


**Fig. 2.** Concentration of thiobarbituric acid reactive substances (TBARS) in the brain extracts 1, 2 or 4 h after exposure to 1, 10 or 100 mg/L SWNT-PEG. The data are expressed as the means ± standard error. *Significant difference ($p < 0.05$) by an orthogonal contrast ($n = 5$).

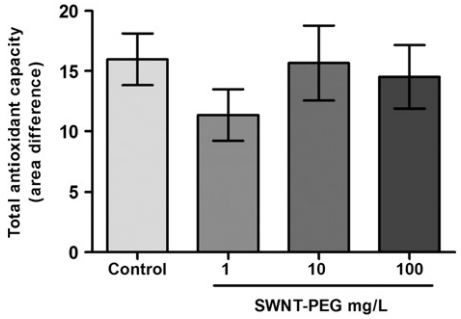


**Fig. 3.** Total antioxidant capacity against peroxyl radicals in brain extracts after 4 h of exposure to 1, 10 or 100 mg/L SWNT-PEG. The data are expressed as the means ± standard error ($n = 5$). Higher bars indicate lower total antioxidant capacity against peroxyl radicals.

*Preparation of brain homogenates.* For organ dissection, the fish were sacrificed by immersion in 200–300 mg/L tricaine methanesulfonate, and then, the brains were extracted. The organs were homogenized (1:3) in Tris–HCl buffer (100 mM, pH 7.75) containing EDTA (2 mM) and $Mg^{2+}$ (5 mM) and were centrifuged at 10,000*g* for 20 min at 4 °C, and the supernatant was exposed to SWNT-PEG (Ferreira et al., 2012). This supernatant was used for the measurement of lipid peroxidation, GSH (reduced glutathione) content, GCL (glutathione-cysteine ligase) activity and total antioxidant capacity. Before the biochemical analysis, the total protein content was determined through the Biuret method (Doles, Brazil) using a microplate reader (BioTek LX 800).

*Exposure to SWNT-PEG.* The brain extracts were exposed *in vitro* for 1, 2 or 4 h to SWNT-PEG (1, 10 or 100 mg/L) in dark conditions at 28 °C. These concentrations were selected based on other *in vitro* studies performed with PC12 cells (Zhang et al., 2011). The untreated control group

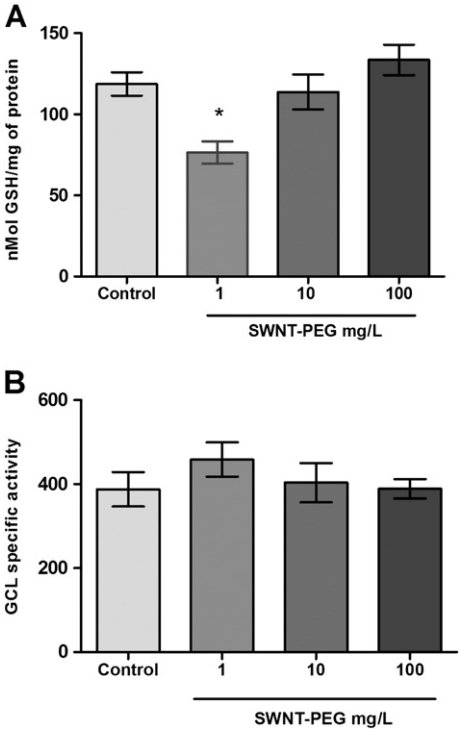


**Fig. 4.** A) Reduced glutathione (GSH) content in brain extracts after 4 h of exposure to 1, 10 or 100 mg/L SWNT-PEG. The data are expressed as the means ± standard error. *Significant difference ($p > 0.05$). B) Glutathione-cysteine ligase (GCL)-specific activity in brain extracts after 4 h of exposure to 1, 10 or 100 mg/L SWNT-PEG. The data are expressed as the means ± SEM (n = 5).

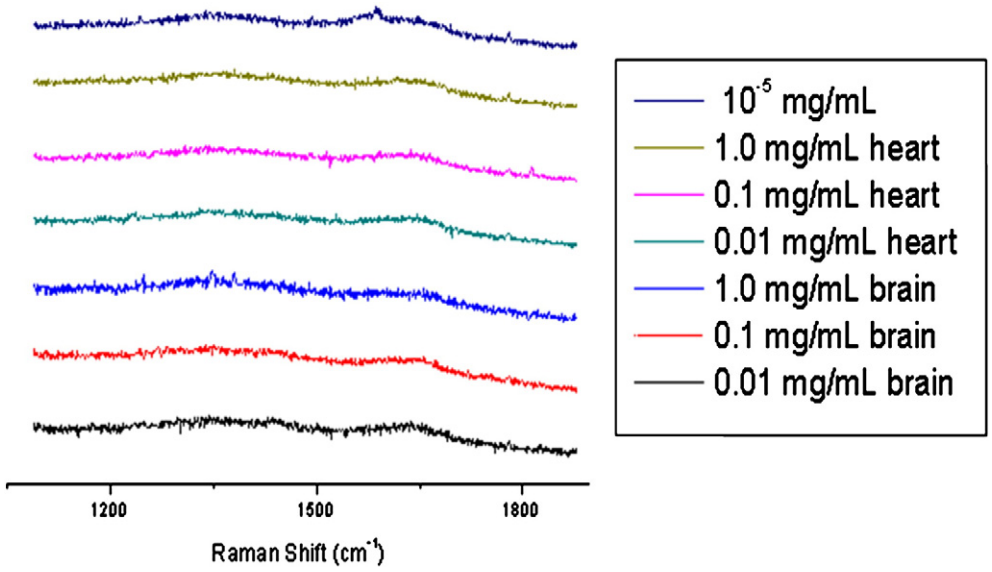


**Fig. 5.** Raman spectra of *Danio rerio* organs after the injections of SWNT-PEG dispersions at different concentrations. The first line depicts a positive control of SWNT-PEG.

was also run in parallel. After each exposure time, the aliquots were stored at −80 °C for further biochemical analysis.

*Measurement of biochemical parameters.* The lipid oxidative damage was assessed through the thiobarbituric acid reactive substances (TBARS) fluorimetric assay (Oakes and Van Der Kraak, 2003). This method is based on the reaction of the most abundant final product of lipid peroxidation, malondialdehyde, with thiobarbituric acid in an acidic medium, which forms a fluorescent complex with excitation and emission at 515 nm and 553 nm, respectively. The readings were carried out in a microplate reader fluorimeter (Perkin Elmer). The concentration of TBARS (nmols/g wet tissue) in the brain samples was calculated by employing a standard curve of tetramethoxypropane (TMP; Acros Organics).

To determine the GCL activity and GSH content in the brain tissue, we followed the method described by White et al. (2003), in which the reaction of naphthalene dicarboxaldehyde (NDA, Invitrogen) with GSH or γ-glutamylcysteine (γ-GC) generates cyclic products that are highly fluorescent (excitation/emission at 485/530 nm). The GCL activity and GSH content of the homogenates were determined by employing a GSH standard curve and were read in a microplate reader fluorimeter (Perkin Elmer).

Finally, the total antioxidant competence against peroxyl radicals was analyzed through ROS determination by employing the fluorogenic compound $H_2$DCF-DA (Invitrogen) in brain homogenates that were

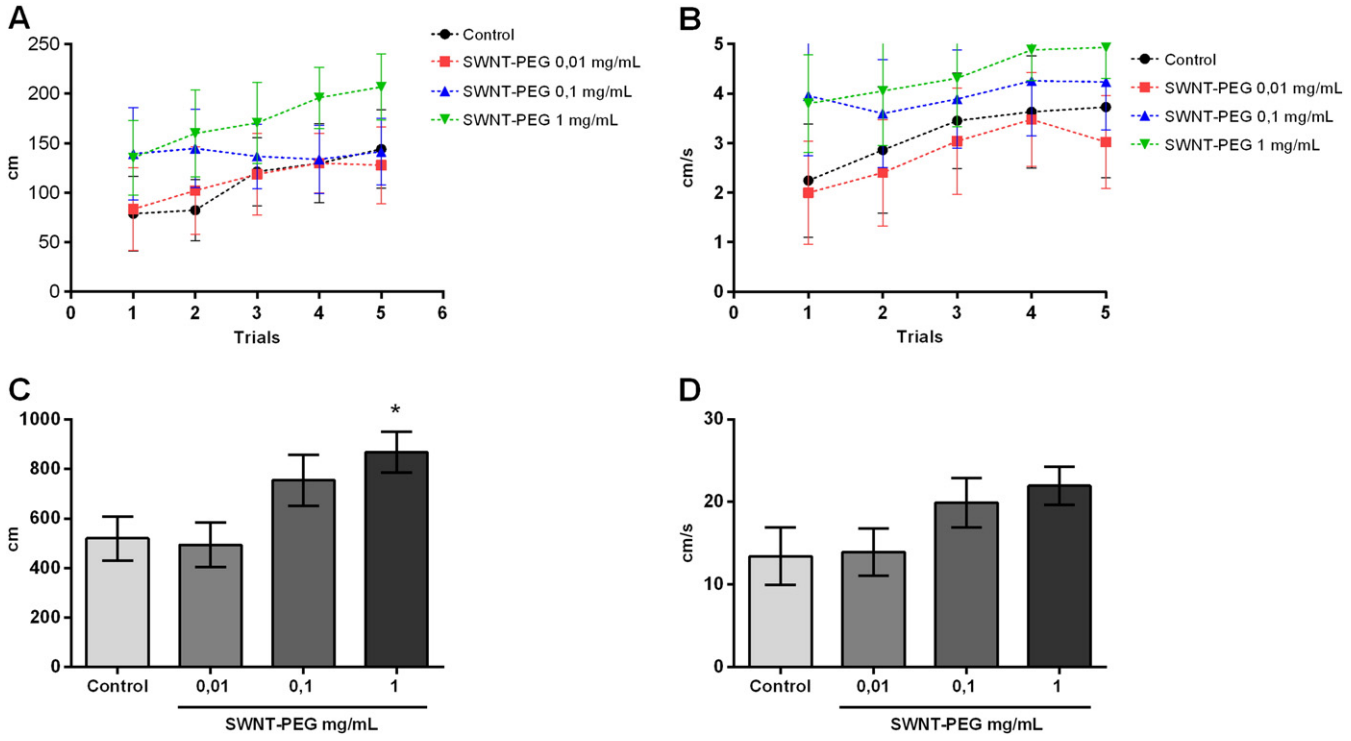


**Fig. 6.** The total distance traveled (A and C) and velocity (B and D) were recorded over 5 min for animals exposed to three concentrations of SWNT-PEG (0.01, 0.1 or 1.0 mg/ml).

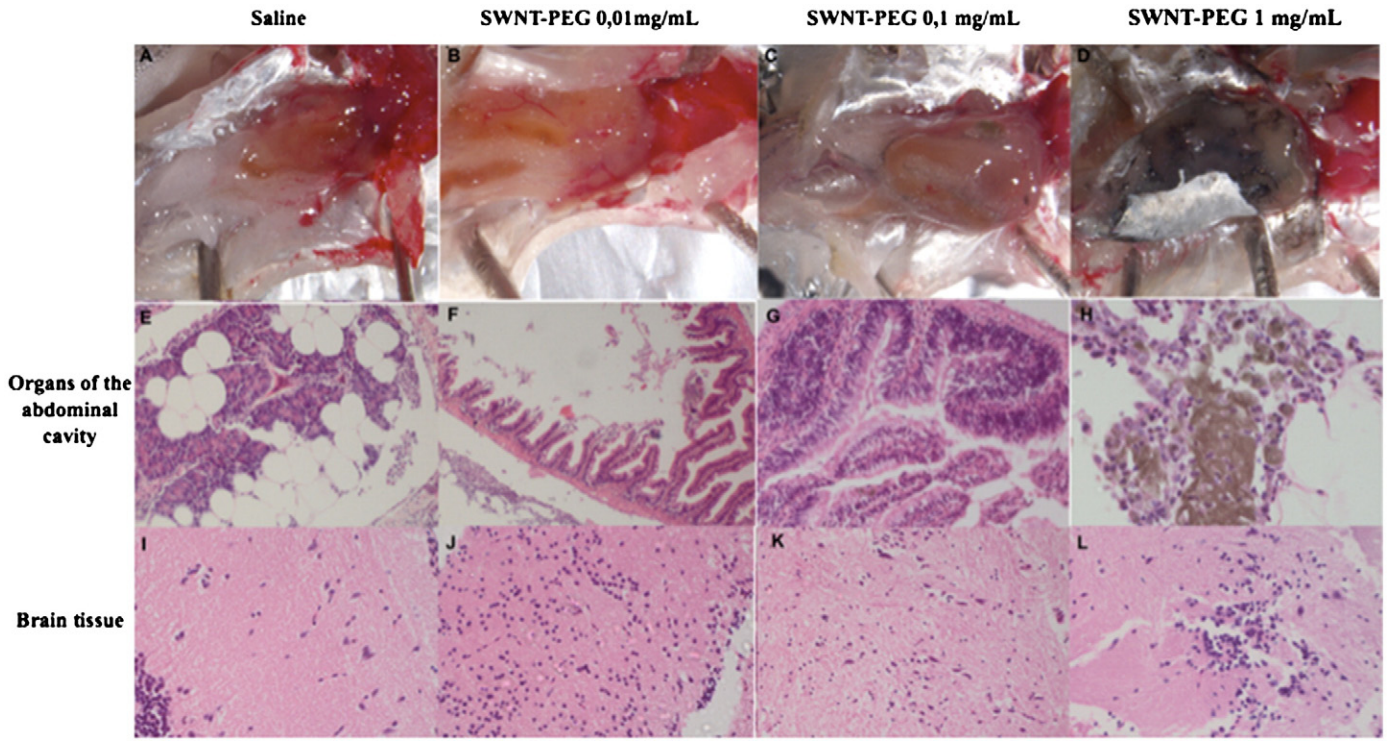


**Fig. 7.** Pictures A, B, C and D are photos of the peritoneal cavity of zebrafish 24 h after the intraperitoneal injection of different concentrations of SWNT-PEG. The other images are slides of zebrafish tissues stained with hematoxylin and eosin. E shows the exocrine pancreas, with a normal acini aspect in the peritoneal fat (20×); F depicts the midgut, with incipient inflammatory infiltrates in the submucosa and dense mononuclear infiltrates in the peritoneum (10×); G shows the intestines, with dense inflammatory infiltrates in the mucosa and submucosa and with superficial mucosal necrosis (40×); and H shows peritoneal tissue with dense inflammatory infiltrates, mainly by macrophages. Melanin deposits were observed in the macrophages (40×); I consists of brain cortex, with slight edema and normal clear cells (40×). J and K are from the cortex, with glial proliferation and focal edema (40×), and L shows a brain section with glial proliferation, edema, signs of neuronal distress with nuclear pallor and satellitosis (40×).

untreated or treated with a peroxyl radical generator (2,2′-azobis-2-methylpropionamidine-dihydrochloride, ABAP, 4 mM, Sigma-Aldrich) (Amado et al., 2009). The readings were carried out in a microplate reader fluorimeter (Perkin Elmer) at excitation and emission wavelengths of 485 and 530 nm, respectively.

### *In vivo experiments*

*Biodistribution of SWNT-PEG.* For this experiment, adult male zebrafish were employed (described in Animals and Housing Section). The animals were injected intraperitoneally with a total of five doses of 10 μl of SWNT-PEG at different concentrations (0.01 mg/ml, 0.1 mg/ml or 1.0 mg/ml) on alternate days. The control group received saline. Forty-eight hours after the last injection, all the animals were sacrificed by immersion in 200–300 mg/L tricaine methanesulfonate for the subsequent tissue removal. For the biodistribution assays, only the brain and heart tissues were used, as the other organs were immersed in SWNT-PEG during the intraperitoneal injection. After removal, the tissues were homogenized in a lysis buffer (1% SDS, 1% Triton X-100, 40 mM Tris acetate, 10 mM EDTA, 10 mM DTT) through homogenization and sonication (1 min for each sample) (Liu et al., 2008). Shortly before the analysis in the equipment (Horiba T 64000 Raman spectrometer, laser excitation wavelength = 785 nm), the tissues were heated at 70 °C for 2 h to obtain a clear lysate for Raman spectroscopy readings.

*Open field test.* The behavioral task was performed using an open field test. The apparatus consisted of a large rectangular opaque glass tank (12.3 cm height × 38.7 cm width × 47.3 cm length) filled with aquarium water to the level of 12 cm (Stewart et al., 2012). In the test session, 42 adult male zebrafish (Animals and Housing Section) were used. The animals were divided into groups as follows: saline (n = 9), 0.01 mg/ml SWNT-PEG (n = 11), 0.1 mg/ml SWNT-PEG (n = 11) and 1 mg/ml SWNT-PEG (n = 11). The animals received intraperitoneal injections of 10 μl of SWNT-PEG 24 h before the test, and the tests were performed in the morning.

The fish were placed into the tank and videotaped for 5 min (divided into five separate trials). The trials were recorded with a camera (Sony

**Table 1**
Semi-quantitative score for analyses of histopathologic features of fish tissues and organs. Each pathological feature was given a score of 0–3.

| | | Score | | | |
|---|---|---|---|---|---|
| Organs or tissues | Pathological feature | 0 | 1 | 2 | 3 |
| Intestine | Inflamatory infiltrates cells | 0/40× field | <2/40× field | 2–5/40× field | >5/40× field |
| | Necrosis | None | Rare and focal | Moderate | Abundant |
| Intraperitoneal space | Peritoneal inflamatory cells | 0/40× field | <2/40× field | 2–5/40 × field | >5/40× field |
| | Peritonealmelanin | None | Small focal melanin | Moderate melanin | Abundant melanin |
| Brain | Edema | None | Focal | Moderate | Severe |
| | Glial proliferetion | None | Small, focal area | Moderate | Severe |
| | Cells with neural distress | 0/40× field | <2/40 × field | 2–5/40× field | >5/40× field |
| | Cells with satelitosis | 0/40× field | <2/40× field | 2–5/40× field | >5/40× field |

Handycam DCR-SR47, New York, NY) and were analyzed off-line using Ethovision XT7 (Noldus IT, Wageningen, Netherlands). Later, we analyzed the mean velocity (cm/s) and distance traveled (cm).

*Histological examination.* The animals were injected using the same protocol employed for the biodistribution assay. Forty-eight hours after the last injection, the animals were sacrificed by immersion in tricaine methanesulfonate (200–300 mg/L) for the subsequent tissue removal (organs of the abdominal cavity and brain). The organs were then collected and fixed in 4% neutral buffered formalin, processed routinely into paraffin, sectioned at 7 μm and stained with hematoxylin and eosin (H&E). In all the experimental groups, five to eight animals were used, and two histological sections were measured for each fish. The sections were evaluated by a single board-certified medical pathologist.

*Statistical analysis.* In the *in vitro* assays, all variables were analyzed by an analysis of variance (ANOVA) (Stewart et al., 2012). The assumptions of normality and homogeneity of variances were verified, and when at least one of the assumptions was violated, mathematical transformations were applied. Comparisons between the means were then performed through the Newmann–Keuls *post-hoc* test. Orthogonal contrasts were applied in the TBARS assay (see Fig. 4). In all cases, the type I error probability was fixed at 0.05 ($\alpha = 0.05$).

In the *in vivo* open field test (OFT), the variables were analyzed by repeated-measures ANOVA with a Bonferroni *post-hoc* test. Next, the endpoint values were calculated by taking the sum of the activity that occurred during 1–5 min for each individual fish; these data were then analyzed by a one-way ANOVA, followed by a Newman–Keuls *post-hoc* test. The data are presented as the mean ± standard error of the mean (S.E.M.), with significance set at $p < 0.05$.

To evaluate the microscopic findings of the tissues, a semi-quantitative grading scale adapted from Janovic, Whitley and Palić (2014) was used. The significance of the differences between the histopathology scores was evaluated using the Kruskal–Wallis test, followed by Dunn's *post-hoc* test. The data are presented as the mean ± S.E.M., with significance set at $p < 0.05$.

## Results and discussion

To understand the activity of carbon nanotubes in biological systems both *in vitro* and *in vivo*, the physicochemical features (i.e., surface functionalization, metallic contaminants, size and aggregation state) of the nanomaterials used in the experiments must be considered (Warheit, 2008; Firme and Bandaru, 2010). Low-resolution TEM analyses revealed that commercial PEG-functionalized SWNT material formed large aggregates in water, even after prolonged bath sonication. The sample contained a large amount of metallic catalyst as well as some graphitic impurities (Fig. 1). The concentration of the final dispersion was estimated by measuring the intensity of light absorption at 700 nm. A concentration of 2.1 ± 0.2 mg/ml was obtained after the entire process.

The SWNTs in the aqueous dispersion were found to exhibit a Zeta potential of approximately −60 mV. This result may be an indication that the PEG-functionalized nanotubes still contained many unreacted carboxylic acid groups (–COOH). Indeed, the Zeta potential of the SWNT-PEG decreased to approximately −30 mV with increasing NaCl concentration (up to 0.06 mol/L), indicating a screening of repulsive forces, as would be expected for charged particles.

Due to their relatively high negative Zeta potential, we expected that the SWNT-PEG hybrids would be vulnerable to aggregation in biological systems because physiological fluids contain a mixture of salts, proteins and other macromolecules that can interact with negatively charged nanoparticle surfaces. Nance et al. (2012) demonstrated that nanoparticles with Zeta potentials less negative than −4 mV were able to diffuse throughout the nervous tissues of rats; however, particles with Zeta potentials lower than −6 mV were unable to diffuse through the same tissues. All of these complex interactions between nanoparticles and biological media constituents must be taken into account by performing *in vitro* analyses before performing studies *in vivo*.

To assess their intrinsic behavior in biological environments *in vitro*, we introduced different concentrations of SWNT-PEG to the homogenized brain tissue of zebrafish and evaluated representative oxidative stress parameters to verify the interactions of these nanostructures with biomolecules. In toxicological evaluations, there are a number of different results that depend on the synthesis method and the physicochemical characteristics of the nanomaterial (Heister et al., 2010).

Furthermore, certain properties, such as surface coating and solubility, may decrease or amplify the size effect, and the size, shape and aggregation are nanomaterial characteristics that can elicit reactive oxygen species (ROS) generation (Suh et al., 2009). Oxidative stress is possibly the main mechanism of nanomaterial toxicity, resulting in damage to lipids, proteins and DNA (Jones, 2006).

We assessed lipid peroxidation as a sensible indicator of the injury level caused by ROS production (Jones, 2006). We observed a significant decrease ($p < 0.05$) in lipid peroxidation after exposure of the homogenized tissue to 1 mg/L SWNT-PEG for 4 h compared to the control group (Fig. 2). Wang et al. (2011) demonstrated that there was a significant increase in the levels of MDA in PC12 cells treated with different concentrations of SWNTs, which occurred in a time- and dose-dependent manner. This difference may be because the SWNTs used in this work were functionalized with PEG; similar nanomaterials were used in another study with PC12 cells in which the authors demonstrated that functionalization with PEG significantly reduces the side effects of SWNTs as well as the disturbance of oxidative stress-related gene expression (Zhang et al., 2011).

Among the oxidative stress parameters studied in the tissue homogenates, we chose a time exposure of 4 h because the time condition was the only one for which a significant modulation in lipid peroxidation was observed. The next parameter analyzed was the total antioxidant capacity, which demonstrated no significant change ($p > 0.05$) (Fig. 3). These results indicate that the presence of SWNT-PEG did not disturb the antioxidant defense system in the brain homogenates.

We also analyzed the GSH content, as GSH is a major intracellular low-molecular-weight thiol compound that plays a critical role in the cellular defense against oxidative stress through scavenging of ROS directly or indirectly in cells (Halliwell and Gutteridge, 2001), and GCL activity, as GCL is the enzyme responsible for catalyzing the synthesis of GSH (Maher, 2006). Our results indicated a significant decrease in the GSH content of the extract exposed to lower concentrations of SWNT-PEG (Fig. 4), a finding that agreed with the results of other studies (Zhang et al., 2011; Valko et al., 2007). The depletion of GSH content induced by SWNT-PEG may be due to an increased production of reactive oxygen species (ROS). However, the other results of our study suggested that this increase in ROS was not sufficient to cause lipid damage in the brain extract and did not increase the activity of GCL (Fig. 4).

In addition to the *in vitro* analysis, an *in vivo* study was conducted. We evaluated the biodistribution of the nanomaterial by Raman spectroscopy; however, if the SWNT-PEG was distributed throughout the zebrafish organs, it reached tissues at concentrations below $10^{-5}$ mg/ml (Fig. 5), as the Raman spectra of the SWNT-PEG G band was not observed in the brain tissues. The SWNT-PEG G band was observed in the control samples with SWNT-PEG concentrations as low as $10^{-5}$ mg/ml. Another study, which was performed using mice and SWNTs noncovalently functionalized with different PEG chains, also did not observe the distribution of these nanomaterials to the brain. This study also assessed particle distribution in the blood, liver and spleen, among other sites, and in these tissues, the presence of PEGylated SWNTs was verified (Liu et al., 2008).

To assess the indirect toxic whole-body effects caused by the nanotubes, we conducted an open field test on animals 24 h after exposure to different concentrations of SWNT-PEG. Locomotor and exploratory activities were evaluated in this test. Only the animals exposed to the

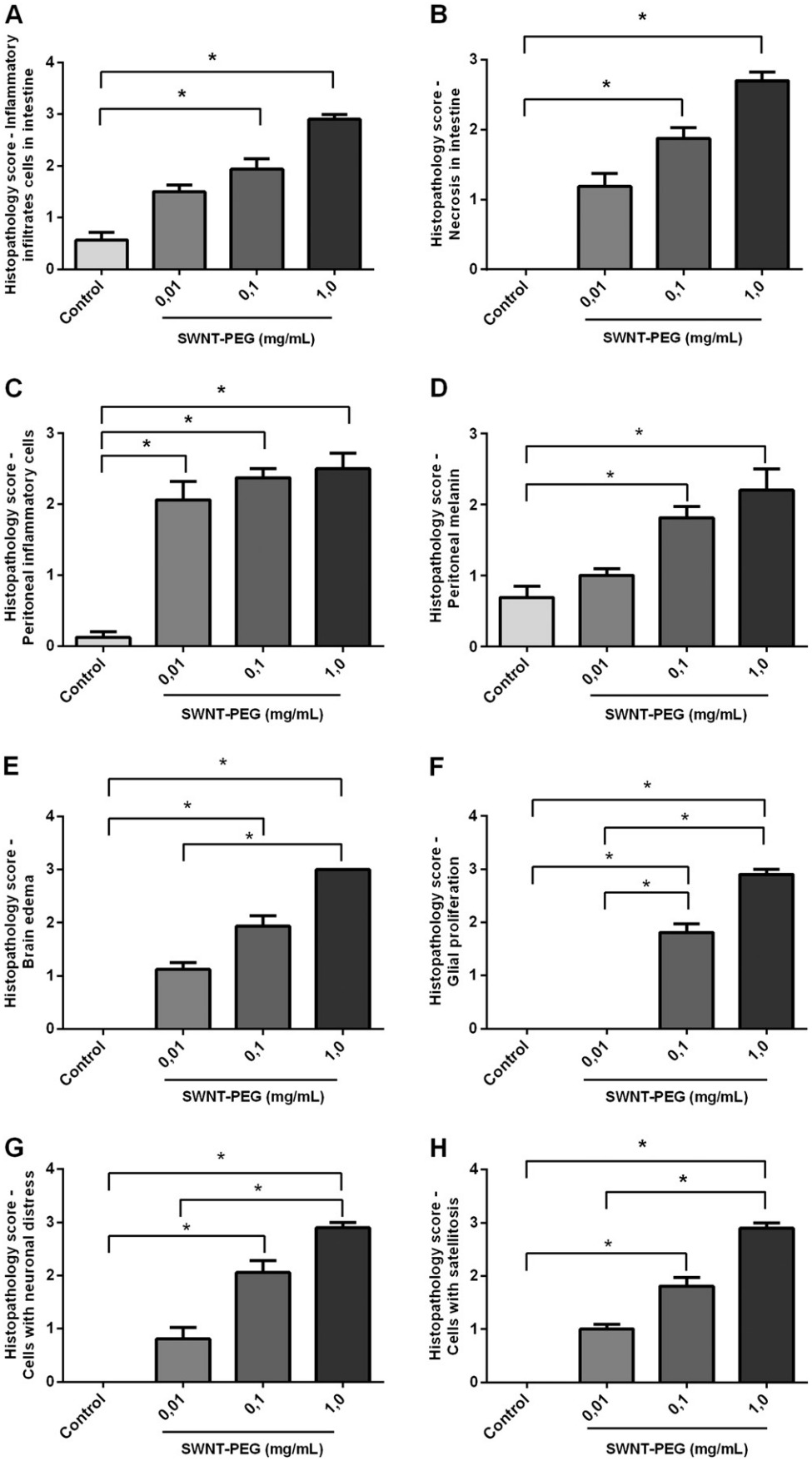
A
Histopathology score - Inflammatory infiltrates cells in intestine
B
Histopathology score - Necrosis in intestine
C
Histopathology score - Peritoneal inflammatory cells
D
Histopathology score - Peritoneal melanin
E
Histopathology score - Brain edema
F
Histopathology score - Glial proliferation
G
Histopathology score - Cells with neuronal distress
H
Histopathology score - Cells with satellitosis
Control
0,01
0,1
1,0
SWNT-PEG (mg/mL)
*

highest concentration of SWNT-PEG (1 mg/ml) demonstrated a significant increase in the overall distance traveled (Fig. 6). Truong et al. (2012) also observed abnormalities in the locomotor activity of animals exposed to gold nanoparticles, supporting the validity of this test for monitoring changes in the central nervous system.

Histological changes in the animals that received intraperitoneal injections of SWNT-PEG were also analyzed (Fig. 7). In this experiment, we observed increased tissue injury and inflammation in a dose-dependent manner. In the abdominal cavity organs, we observed injuries caused by direct tissue interaction with the nanomaterial. Although nervous tissue damage occurred in an indirect way because no SWNT-PEG was found in the brain, the animals presented an inflammatory response, as demonstrated by the histological analysis. Furthermore, the analysis of the semi-quantitative histopathology scoring of the tissues (Table 1) shows differences between the control group and the treatments, as shown in Fig. 8. These data show, in a dose-dependent manner, an increase in inflammatory infiltrate cells in the intestine (A), necrosis in the intestine (B), peritoneal inflammatory cells (C), peritoneal melanin (D), brain edema (E), glial proliferation (F), cells with neuronal distress (G) and cells with satellitosis (H). These results are congruent with a study using fathead minnow, where intraperitoneal injection of hydroxylated fullerenes was reported to induce hepatic and renal tissue injury, with dose-dependent tissue injury and higher cumulative histopathology scores as well (Janovic´, Whitley and Palic´ 2014).

The results obtained in this study demonstrated that the SWNT-PEG caused toxicity due to its lack of biocompatibility *in vivo*, which may compromise its use for biomedical proposes. The *in vitro* experiment showed that the SWNT-PEG produced changes in the oxidative stress parameters analyzed, with a discrete antioxidant effect on lipid peroxidation and an opposite pro-oxidant effect, as indicated by the depletion of GSH. Additionally, it is important to consider the influence of contaminants present in the SWNT-PEG sample, such as Yttrium (Y) and Nickel (Ni). Jakubek and co-workers have shown that these metals are capable of inhibiting calcium channels, which could be the mechanism responsible for a variety of toxic effects related to these metals (Jakubek et al, 2009).

It is possible to conclude that these nanomaterials have some limitations. As demonstrated by the *in vivo* study, the SWNTs functionalized with PEG 600 were not able to distribute to other organs, most likely due to their instability in saline medium. In a biological medium, the aggregation of the nanotubes was observed and resulted in damage to blood vessels, leading to thrombus formation and eventual tissue necrosis. Thus, an extensive inflammatory process occurred once the nanomaterials were trapped in the abdominal cavity after injection. Additionally, in the central nervous system, several histological modifications were observed in addition to the behavioral changes observed in the open field test. However, because these nanomaterials are promising in the biomedical area, further studies are necessary, especially with SWNTs functionalized with larger PEG chains and denser PEG coatings.

## Acknowledgments

This work was supported by Programa de Núcleos Emergentes (PRONEM/FAPERGS) (11/2037-9), DECIT/SCTIE-MS through Conselho Nacional de Desenvolvimento Científico e Tecnológico (CNPq) and Fundação de Amparo à Pesquisa do Estado do Rio Grande do Sul (FAPERGS, Proc. 10/0036-5-PRONEX/Conv. 700545/2008), Nanotoxicology Network (MCTI/CNPq process number 552131/2011-3) and Instituto Nacional de Ciência e Tecnologia de Nanomateriais de Carbono (INCT-NanoCNPq). Daniela Martí Barros is a research fellow from CNPq, and Gisele Eva Bruch Weber received a graduate fellowship from Coordenação de Aperfeiçoamento de Pessoal de Nível Superior (CAPES).

## References

Ajayan, P.M., 1999. Nanotubes from carbon. Chem. Rev. 99 (7), 1787–1800.
Amado, L.L., Garcia, M.L., Ramos, P.B., Freitas, R.F., Zafalon, B., Ferreira, J.L.R., Yunes, J.S., Monserrat, J.M., 2009. A method to measure total antioxidant capacity against peroxyl radicals in aquatic organisms: application to evaluate microcystins toxicity. Sci. Total Environ. 407, 2115–2123.
Barros, T.P., Alderton, W.K., Reynolds, H.M., Roach, A.G., Berghmans, S., 2008. Zebrafish: an emerging technology for in vivo pharmacological assessment to identify potential safety liabilities in early drug discovery. Br. J. Pharmacol. 154 (7), 1400–1413.
Bekyarova, E., Ni, Y., Malarkey, E.B., Montana, V., McWilliams, J.L., Haddon, R.C., Parpura, V., 2005. Applications of carbon nanotubes in biotechnology and biomedicine. J. Biomed. Nanotechnol. 1 (1), 3–17.
Cheng, J., Chan, C.M., Veca, L.M., Poon, W.L., Chan, P.K., Qu, L., Sun, Y.P., Cheng, S.H., 2009. Acute and long-term effects after single loading of functionalized multi-walled carbon nanotubes into zebrafish (*Danio rerio*). Toxicol. Appl. Pharmacol. 235 (2), 216–225.
Cheung, W., Pontoriero, F., Taratula, O., Chen, A.M., He, H., 2010. DNA and carbon nanotubes as medicine. Adv. Drug Deliv. Rev. 62 (6), 633–649 (Review).
de Castro, M.R., Lima, J.V., de Freitas, D.P., Valente Rde, S., Dummer, N.S., de Aguiar, R.B., dos Santos, L.C., Marins, L.F., Geracitano, L.A., Monserrat, J.M., Barros, D.M., 2009. Behavioral and neurotoxic effects of arsenic exposure in zebrafish (*Danio rerio*, Teleostei: Cyprinidae). Comp. Biochem. Physiol. C: Toxicol. Pharmacol. 150 (3), 337–342.
Fako, V.E., Furgeson, D.Y., 2009. Zebrafish as a correlative and predictive model for assessing biomaterial nanotoxicity. Adv. Drug Deliv. Rev. 61 (6), 478–486.
Ferreira, J.L.R., Barros, D.M., Geracitano, L.A., Fillmann, G., Fossa, C.E., Almeida, E.A., Prado, M.C., Neves, B.R.A., Pinheiro, M.V.B., Monserrat, J.M., 2012. In vitro exposure to fullerene c60 influences redox state and lipid peroxidation in brain and gills from *cyprinus carpio* (cyprinidae). Environ. Toxicol. Chem. 31 (5), 961–967.
Firme, C.P., Bandaru, P.R., 2010. Toxicity issues in the application of carbon nanotubes to biological systems. Nanomedicine: NBM 6, 245–256.
Foldvari, M., Bagonluri, M., 2008. Carbon nanotubes as functional excipients for nanomedicines: II. Drug delivery and biocompatibility issues. Nanomedicine 4 (3), 183–200.
Galvan-Garcia, P., Keefer, E.W., Yang, F., Zhang, M., Fang, S., Zakhidov, A.A., Baughman, R. H., Romero, M.I., 2007. Robust cell migration and neuronal growth on pristine carbon nanotube sheets and yarns. J. Biomater. Sci. Polym. Ed. 18 (10), 1245–1261.
Gilmore, J.L., Yi, X., Quan, L., Kabanov, A.V., 2008. Novel nanomaterials for clinical neuroscience. J. NeuroImmune Pharmacol. 3, 83–94 (Review).
Halliwell, B., Gutteridge, J.M.C., 2001. Role of free radicals in the neurodegenerative disease: therapeutic implications for antioxidant treatment. Drugs Aging 18, 685–716.
Heister, E., Lamprecht, C., Neves, V., Tilmaciu, C., Datas, L., Flahaut, E., Soula, B., Hinterdorfer, P., Coley, H.M., Silva, S.R.P., McFadden, J., 2010. Higher dispersion efficacy of functionalized carbon nanotubes in chemical and biological environments. ACS Nano 4 (5), 2615–2626.
Ilbasmiş-Tamer, S., Yilmaz, S., Banoğlu, E., Değim, I.T., 2010. Carbon nanotubes to deliver drug molecules. J. Biomed. Nanotechnol. 6 (1), 20–27.
Jain, S., Thakare, V.S., Das, M., Godugu, C., Jain, A.K., Mathur, R., Chuttani, K., Mishra, A.K., 2011. Toxicity of multiwalled carbon nanotubes with end defects critically depends on their functionalization density. Chem. Res. Toxicol. 24 (11), 2028–2039.
Jakubek, L., Marangoudakis, S., Raingo, J., Liu, X., Lipscombe, D., Hurt, R., 2009. The inhibition of neuronal calcium ion channels by trace levels of yttrium released from carbon nanotubes. Biomaterials 30 (31), 6351–6357.
Janovic´, B., Whitley, E.M., Palic´, D., 2014. Histopathology of feathed minnow(Pimephales promelas) exposed to hidroxyated fulerenes. Nanotoxicol. 8 (7), 755–763.
Johnston, H.J., Hutchison, G.R., Christensen, F.M., Peters, S., Hankin, S., Aschberger, K., Stone, V., 2010. A critical review of the biological mechanisms underlying the in vivo and in vitro toxicity of carbon nanotubes: the contribution of physico-chemical characteristics. Nanotoxicology 4 (2), 207–246.
Jones, D.P., 2006. Redefining oxidative stress. Antioxid. Redox Signal. 8, 1865–1879.
Kalinina, I., Worsley, K., Lugo, C., Mandal, S., Bekyarova, E., Haddon, R.C., 2011. Synthesis, dispersion, and viscosity of poly(ethylene glycol)-functionalized water-soluble single-walled carbon nanotubes. Chem. Mater. 23, 1246–1253.
Kam, N.W., O'Connell, M., Wisdom, J.A., Dai, H., 2005. Carbon nanotubes as multifunctional biological transporters and near-infrared agents for selective cancer cell destruction. Proc. Natl. Acad. Sci. U. S. A. 102 (33), 11600–11605.
Kang, B., Yu, D., Dai, Y., Chang, S., Chen, D., Ding, Y., 2009. Biodistribution and accumulation of intravenously administered carbon nanotubes in mice prprobed by Raman spectroscopy and fluorescent labeling. Carbon 47 (4), 1189–1192.
Liang, F., Chen, B., 2010. A review on biomedical applications of single-walled carbon nanotubes. Curr. Med. Chem. 17 (1), 10–24.
Linney, E., Upchurch, L., Donerly, S., 2004. Zebrafish as a neurotoxicological model. Neurotoxicol. Teratol. 27 (1), 709–718.

**Fig. 8.** Histopathology scores. The semi-quantitative scores are representative of histopathologic features in the control and SWNT-PEG treatments. Comparisons of the mean histopathology scores for inflammatory infiltrate in the cells of the intestine (A), necrosis in the intestine (B), peritoneal inflammatory cells (C), peritoneal melanin (D), brain edema (E), glial proliferation (F), cells with neuronal distress (G) and cells with satellitosis (H) are shown. Values are expressed as the means ± SEM, n = 5–8. $^{*}p < 0.05$ for a statistically significant effect (Kruskal–Wallis test, followed by Dunn's *post-hoc* test).

Liopo, A.V., Stewart, M.P., Hudson, J., Tour, J.M., Pappas, T.C., 2006. Biocompatibility of native and functionalized single-walled carbon nanotubes for neuronal interface. J. Nanosci. Nanotechnol. 6 (5), 1365–1374.
Liu, Z., Davis, C., Cai, W., He, L., Chen, X., Dai, H., 2008. Circulation and long-term fate of functionalized, biocompatible single-walled carbon nanotubes in mice probed by Raman spectroscopy. Proc. Natl. Acad. Sci. U. S. A. 105 (5), 1410–1415.
Liu, Z., Tabakman, S.M., Chen, Z., Dai, H., 2009. Preparation of carbon nanotube bioconjugates for biomedical applications. Nat. Protoc. 4 (9), 1372–1382.
Maher, P., 2006. Redox control of neural function: background, mechanisms, and significance. Antioxid. Redox Signal. 8 (11-12), 1941–1970.
Mattson, M.P., Haddon, R.C., Rao, A.M., 2000. Molecular functionalization of carbon nanotubes and use as substrates for neuronal growth. J. Mol. Neurosci. 14 (3), 175–182.
Medina, C., Santos-Martinez, M.J., Radomski, A., Corrigan, O.I., Radomski, M.W., 2007. Nanoparticles: pharmacological and toxicological significance. Br. J. Pharmacol. 50 (5), 552–558.
Meng, L., Zhang, X., Lu, Q., Fei, Z., Dyson, P.J., 2012. Single walled carbon nanotubes as drug delivery vehicles: targeting doxorubicin to tumors. Biomaterials 33 (6), 1689–1698.
Naderi, N., Madani, S.Y., Mosahebi, A., Seifalian, A.M., 2013. Carbon nanotubes in the diagnosis and treatment of malignant melanoma. Anticancer Agents Med. Chem. 13 (1), 171–185.
Nance, E.A., Woodworth, G.F., Sailor, K.A., Shih, T., Xu, Q., Swaminathan, G., Xiang, D., Eberhart, C., Hanes, J., 2012. Penetration of large polymeric nanoparticles within brain tissue. Nanomedicine 149 (4), 149ra119.
Nel, A., Xia, T., Mädler, L., Li, N., 2006. Toxic potential of materials at the nanolevel. Science 311 (5761), 622–627 (Review).
Oakes, K.D., Van Der Kraak, G.J., 2003. Utility of the TBARS assay in detecting oxidative stress in white sucker (Catostomus commersoni) populations exposed to pulp mill effluent. Aquat. Toxicol. 63 (4), 447–463.
Oberdörster, G., Oberdörster, E., Oberdörster, J., 2005. Nanotoxicology: an emerging discipline evolving from studies of ultrafine particles. Environ. Health Perspect. 113, 823–839.
Oberdörster, G., Elder, A., Rinderknecht, A., 2009. Nanoparticles and the brain: cause for concern? J. Nanosci. Nanotechnol. 9 (8), 4996–5007.
Porter, A., Gass, M., Muller, K., Skepper, J., Midgley, P., Welland, M., 2007. Direct imaging of single-walled carbon nanotubes in cells. Nat. Nanotechnol. 2, 713–717.
Roman, J.A., Niedzielko, T.L., Haddon, R.C., Parpura, V., Floyd, C.L., 2011. Single-walled carbon nanotubes chemically functionalized with polyethylene glycol promote tissue repair in a rat model of spinal cord injury. J. Neurotrauma 28 (11), 2349–2362.
Smith, D.M., Mizumori, S.J., 2006. Learning-related development of context-specific neuronal responses to places and events: the hippocampal role in context processing. J. Neurosci. 26 (12), 3154–3163.
Stewart, A.M., Gaikwad, S., Kyzar, E., Kalueff, A.V., 2012. Understanding spatio-temporal strategies of adult zebrafish exploration in the open field test. Brain Res. 1451, 44–52.
Sucapane, A., Cellot, G., Prato, M., Giugliano, M., Parpura, V., Ballerini, L., 2009. Interactions between cultured neurons and carbon nanotubes: a nanoneuroscience vignette. J. Nanoneurosci. 1 (1), 10–16.
Suh, W.H., Suslick, K.S., Stucky, G.D., Suh, Y.H., 2009. Nanotechnology, nanotoxicology, and neuroscience. Prog. Neurobiol. 87, 133–170.
Truong, L., Saili, K.S., Miller, J.M., Hutchison, J.E., Tanguay, R.L., 2012. Persistent adult zebrafish behavioral deficits results from acute embryonic exposure to gold nanoparticles. Comp. Biochem. Physiol. C 155, 269–274.
Valko, M., Leibfritz, D., Moncol, J., Cronin, M.T., Mazur, M., Telser, J., 2007. Free radicals and antioxidants in normal physiological functions and human disease. Int. J. Biochem. Cell Biol. 39 (1), 44–84.
Vashist, S.K., Zheng, D., Pastorin, G., Al-Rubeaan, K., Luong, J.H., Sheu, F.S., 2011. Delivery of drugs and biomolecules using carbon nanotubes. Carbon 49, 4077–4097.
Wang, J., Sun, P., Bao, Y., Liu, J., An, L., 2011. Cytotoxicity of single-walled carbon nanotubes on PC12 cells. Toxicol. in Vitro 25, 242–250.
Warheit, D.B., 2008. How meaningful are the results of nanotoxicity studies in the absence of adequate material characterization? J. Toxicol. Sci. 101, 183–185.
White, C.C., Viernes, H., Krejsa, C.M., Botta, D., Kavanagh, T.J., 2003. Fluorescence-based microtiter plate assay for glutamate–cysteine ligase activity. Anal. Biochem. 318, 175–180.
Yang, S.T., Fernando, K.A., Liu, J.H., Wang, J., Sun, H.F., Liu, Y., Chen, M., Huang, Y., Wang, X., Wang, H., Sun, Y.P., 2008a. Covalently Pegylated carbon nanotubes with stealth character in vivo. Small 4 (7), 940–944.
Yang, S.T., Wang, X., Jia, G., Gu, Y., Wang, T., Nie, H., Ge, C., Wang, H., Liu, Y., 2008b. Long-term acumulation and low toxicity of single wall carbon nanotubes in intravenously exposed mice. Toxicol. Lett. 181 (3), 182–189.
Zhang, Y., Bai, Y., Yan, B., 2010. Functionalized carbon nanotubes for potential medicinal applications. Drug Discov. Today 15, 428–435.
Zhang, Y., Xu, Y., Li, Z., Chen, T., Lantz, S.M., Howard, P.C., Paule, M.G., 2011. Mechanistic toxicity evaluation of uncoated and pegylated single-walled carbon nanotubes in neuronal PC12 cells. ACS Nano 5 (9), 7020–7033.
Zhao, W., Karp, J.M., Ferrari, M., Serda, R., 2011. Bioengineering nanotechnology: towards the clinic. Nanotechnology 22 (49), 490201.